Journal of Chromatography, 488 (1989) 249–265
Biomedical Applications
Elsevier Science Publishers B.V., Amsterdam — Printed in The Netherlands

CHROMBIO. 4552

GAS CHROMATOGRAPHY–MASS SPECTROMETRY OF PERINDOPRIL AND ITS ACTIVE FREE METABOLITE, AN ANGIOTENSIN CONVERTASE INHIBITOR: CHOICE OF DERIVATIVES AND IONIZATION MODES

CHRISTOS TSACONAS

Laboratoire de Biochimie Médicale and Centre de Spectrométrie de Masse, Faculté de Médecine, F-21033 Dijon (France)

MICHÈLE DEVISSAGUET

Institut de Recherches Internationales Servier, F-92202 Neuilly-sur-Seine (France)

and

PRUDENT PADIEU*

Laboratoire de Biochimie Médicale and Centre de Spectrométrie de Masse, Faculté de Médecine, 7 bd Jeanne d'Arc, F-21033 Dijon (France)

SUMMARY

Perindopril, a perhydroindole compound and a novel class of angiotensin convertase inhibitor, after oral administration leads to an active metabolite by de-esterification of an ethyl ester. Routine biological measurements are currently done using a radioimmunological assay, but a mass fragmentographic method was developed using plasma spiked with the drugs, which were then derivatized to the isobutyl ester heptofluorobutyramide and assayed using ammonia negative chemical ionization. Levels of 100 pg/ml were assayed. However, isobutanol derivatization provoked partial transesterification of the ethyl ester of the parent drug into the diisobutyl ester derivative, which corresponds to the active metabolite. A second method of derivatization to stable trimethylsilyl esters preserved the original ethyl ester of the parent drug. Despite the lower ionization yields, the mass fragmentographic method was sensitive and accurate enough to work satisfactorily at the 2 ng/ml level in spiked plasma, which is the level found currently in patients.

INTRODUCTION

Perindopril (S-9490-3, **I**, Fig. 1A), 1-{(2*S*) 2-[(1*S*) 1-carbethoxybutylamino]-1-oxopropyl}-(2*S*,3a*S*,7a*S*)-perhydroindole-2-carboxylic acid, [1] is a novel inhibitor of the enzyme that converts angiotensin I into angiotensin II [2]. On oral administration of the drug, the acid form **I** (Fig. 1A) is de-ethylated under the effect of esterases into the active metabolite **II** (S-9780, Fig. 1B) bearing two free carboxylic groups. We established a sensitive gas chromatographic–mass spectro-

0378-4347/89/$03.50

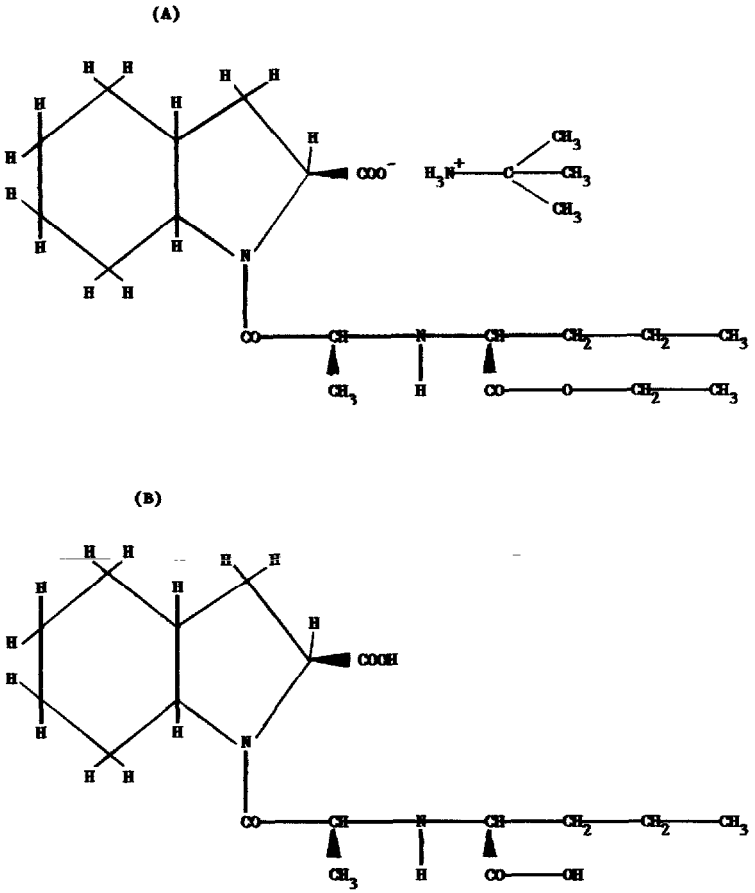

Fig. 1. Structure of Perindropil, S-9490-3, I (A) and its active metabolite S-9780, II (B).

metric (GC–MS) method for the determination of isobutyl ester heptafluorobutyramide (IBHFB) derivatives of **II** and of **III** (S-10841-1), after extraction from plasma using **III**, a structural analogue close to **II**, as an internal standard for quantitation. Mass fragmentography of negative ions using the ammonia chemical ionization mode (NH_3-CI^-) allowed 100 pg/ml to be routinely assessed as the limit of sensitivity was 0.6 pg of **II** injected from a 200 pg/ml solution.

Because the IBHFB derivatization provoked partial transesterification of the ethyl ester of **I** into the isobutyl ester, leading to two compounds, the genuine isobutyl, ethyl diester and the isobutyl diester of **II**, another method of derivatization to the trimethylsilyl ester (TMS) of the sole free carboxylic group(s) was devised. This method of derivatization allowed the simultaneous assay of **I**, the parent plasmatic drug, and free **II**, the active metabolite, using mass fragmentography with methane chemical ionization (CH_3-CI). However, with treated patients the additional presence of the conjugate of the active metabolite necessitated the separation of the three compounds by liquid chromatography followed by assay by radioimmunology [3,4]. In this paper we report GC–MS data for both

derivatives, with emphasis on the fluoro derivative of the amide group and on the use of NH_3-CI^-, which together combine the major advantages of electron impact ionization (EI) and of CI, with a high total ionization yield and the production of intense high-mass ions.

EXPERIMENTAL

Products and reagents

The parent drug **I**, the active metabolite **II** and the internal standard (I.S.) **III** were a gift from Laboratoires Servier (Suresnes, France). Organic solvents and other reagents were obtained from Merck (Darmstadt, F.R.G.) except methanol, which was supplied by Prolabo (Paris, France). Heptafluorobutyryl anhydride (HBFA) was obtained from Pierce Europe (Oud-Beijerland, The Netherlands), N,O-bis(trimethylsilyl)acetamide (BSA) from Supelco (Bellefonte, PA, U.S.A.) and Sep-Pak cartridges of C_{18} bonded phase from Waters Assoc. (Milford, MA, U.S.A.).

Derivatization

Each of **II** and **III** and their mixture were derivatized according to the following methods. A known amount of the reagent was added to the dry residue resulting from evaporation of a standard solution or of an extract from 1–2 ml of plasma (see below) at 45°C and under a stream of dry nitrogen.

Formation of IBHFB derivatives

A known volume (200–500 μl) of dry 4 *M* hydrochloric acid solution in isobutanol (*sec.*-butanol) was added to the dry residue and heated at 110°C for 2 h [5]. After evaporation of the isobutanol at 60°C under a stream of dry nitrogen, a known volume (50 or 100μl) of 20% HFBA in ethyl acetate was added and heated at 90°C for 1 h. The derivatives were stable for at least 3 months in the dark at room temperature.

Formation of TMS derivatives

A known volume (50 or 100 μl) of a mixture of BSA and pyridine (50:50, v/v) was added to the dry residue and heated at 60°C for 2 h. The derivatives were stable for at least 2 months when kept at room temperature in the dark.

Gas chromatography

The conditions of derivatization and for the GC method were established using a Packard Model 427 gas chromatograph (Packard-Becker, Delft, The Netherlands) equipped with a fused-silica capillary column (25 m×0.35 mm I.D.) coated with a film of OV-1 stationary phase of 0.22 μm thickness (Spiral, Couternon-Dijon, France). The carrier gas was dry nitrogen at a flow-rate of 20 ml/min in GC alone and helium at the same flow-rate in the case of GC–MS. The derivatized

sample was injected by means of an all-glass solid injector [6] and monitored using a flame ionization detector. Plasma levels were established by mass fragmentography (MF) using a Ribermag Model GC-MS R10-10C quadrupole mass spectrometer with a SIDAR 150 computer system (Delsi-Nermag, Rueil-Malmaison, France) coupled to a Varian Model 3700 gas chromatograph (Varian, Orsay, France) equipped with the same capillary column. The GC–MS and MF analyses were carried out in the EI, CH_4-CI and NH_3-CI^+ or NH_3-CI^- modes.

Plasma extraction

Extraction was done by liquid–solid chromatography at pH 1 using a Sep-Pak [7] cartridge. Frozen plasma was thawed at room temperature. A known amount of I.S. (10 ng/ml) was added to a known volume of plasma (up to 2 ml), which was diluted with the same volume (2 ml) of 1 *M* hydrochloric acid. The mixture was stirred for 10 s with a vortex mixer and then centrifuged at 6500 *g* for 15 min. The Sep-Pak cartridge was washed with 6 ml of methanol delivered with a glass syringe and then with 6 ml of 0.5 *M* hydrochloric acid. The centrifuged supernatant liquid was passed through the cartridge at a rate of 2 ml/min. The cartridge was then washed with 12 ml of distilled water, dried with dry nitrogen for 30 s and, finally, extracted with 8 ml of methanol at the same flow-rate using a glass syringe. The eluted fractions were evaporated at 45 °C under a stream of dry nitrogen and the dry residues were taken up in the derivatization reagent. Extraction yields were established.

Method of plasma assay

A pool of human plasma specimens was first assayed without drug addition to test the presence of any contaminants or interfering drugs. Spiked aliquots of plasma were extracted immediately or were kept at −20 °C until extraction and analysis. The calculation of the amount of **I** and **II** was made from at least two MF analyses per sample after verifying the linearity of response. The response factor k_1 was calculated from peak areas of selected m/z ions, the base peak and the highest most intense ion. The latter was $[(M+H)-3\times FH]^-$ for IBHFB derivatives or $[M+H]^+$ for TMS derivatives. Four calibration graphs (CG-1 to CG-4) were drawn from k_i established from plasma samples spiked with various amounts of **I** and **II** versus two different amounts of I.S. (**III**): 1 ng/ml I.S. for CG-1, from 100 pg to 50 ng **I** and **II** per ml of plasma; and 10 ng/ml I.S. for CG-2, from 10 pg to 500 ng, for CG-3, from 2 to 100 ng, and for CG-4, from 5 to 500 ng of **I** and **II** per ml of plasma.

RESULTS AND DISCUSSION

Fluorinated derivatives

Owing to the need to determine down to 0.5 ng/ml of drug in plasma, it was first hypothesized that MF should be performed on fluoro derivatives using the

chemical ionization mode. Among a series of derivatives assayed trifluoroacetamide–trifluoroethanol ester, trifluoroacetamide–isobutanol ester and heptafluorobutyramide–isobutanol ester, the last derivative was found to be the best with respect to yield, sensitivity and formation of high-mass compounds devoided of coeluted plasma contaminants.

Gas chromatography

Fig. 2 show that the IBHFB derivative of the I.S., **III**-IBHFB, was eluted first and then the active metabolite **II**-IBHFB, as a unique peak from the OV-1 fused-silica capillary column. The retention times were 6 min 12 s and 7 min 42 s, respectively, at a carrier gas (nitrogen) flow-rate of 20 ml/min and a temperature gradient of 2°C/min starting at 230°C.

Gas chromatography–mass spectrometry

In the EI mode the two compounds were highly cleaved. The base peaks corresponded to the perhydroindole ring arising from cleavage i (Fig. 3A), the m/z ions of 123 (Fig. 3A) and 109 (Fig. 3B), respectively. The only notable peak with a relatively high mass was the ion of m/z 340 arising from that of m/z 396 (cleavage e) by the loss of *sec.*-butene (cleavage sb1), $340 = [396 - (56 - H)]^+$, exhibiting relative intensities (RI) of 22% and 29%, respectively. In the NH_3-CI^+ mode the adduct ions $[M+H]^+$, $m/z = 635$, of **III**-IBHFB (RI = 15%) and 649 of **II**-IBHFB (RI = 50%) appeared interesting to be selected for MF (see Table I), but no other high-mass ions with high relative intensity were produced for ions M^+ with m/z between 268 for **III**-IBHFB and 282 for **II**-IBHFB. These two ions resulted from the same type of cleavage $[(M+H) - (c-H)]^+$ (Table I). In the NH_3-CI^- mode, the butyramide bond was not cleaved and the mass spectra

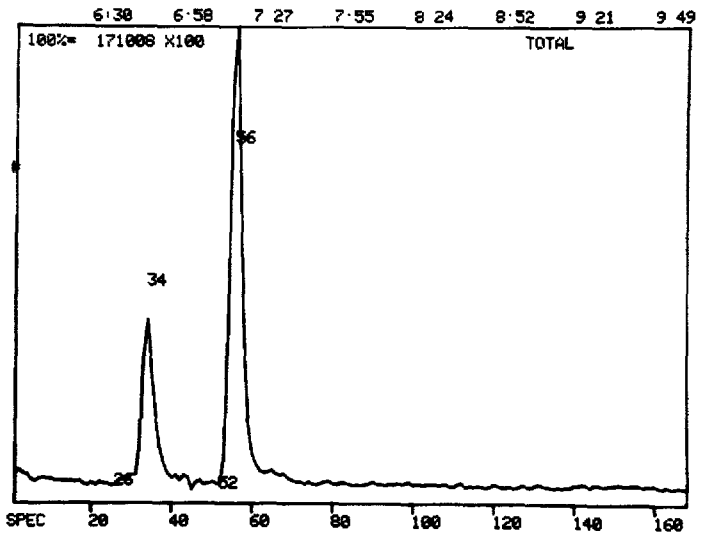

Fig. 2. Gas chromatography of **III**-IBHFB (internal standard) and **II**-IBHFB (active metabolite): 1st peak, **III**-IBHFB; 2nd peak, **II**-IBHFB. Fused-silica capillary column (25 m); temperature programmed at 4°C/min from 200°C; pressure (helium), 0.7 bar.

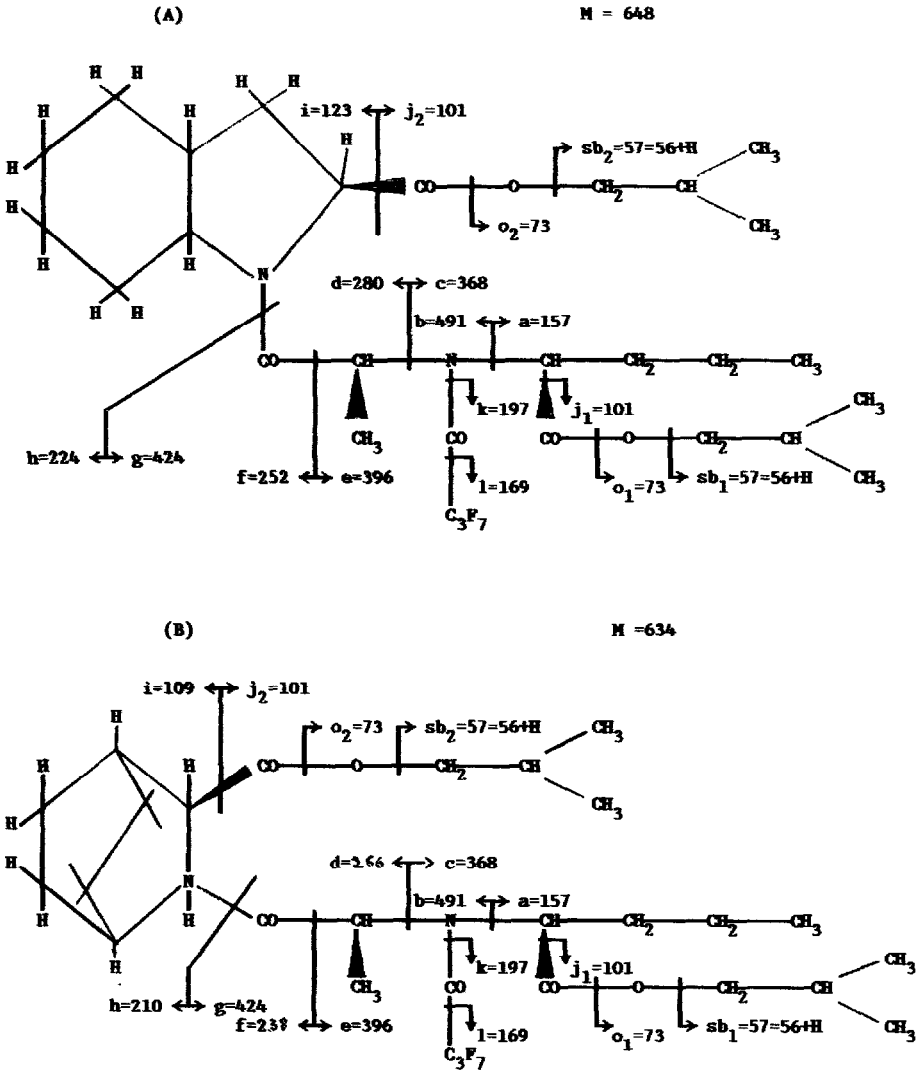

Fig. 3. Structure and fragmentation of **II** (A) and **III** (B) as IBHFB derivatives.

displayed a large number of peaks. Fig. 4 shows the mass spectrum of **II**-IBHFB. Table I lists the characteristic ions produced by **II**-IBHFB and **III**-IBHFB, in the NH_3-CI^- mode. The fragmentation pathways of **II**-IBHFB and **III**-IBHFB, were unambiguously established by comparing identical ions arising from the cleaved side-chain and homologous ions from the cleaved perhydroindole moiety, therefore exhibiting a 14 a.m.u. difference in favour of **I**-IBHFB. Therefore, the fragmentation pathway of **II**-IBHFB consisted of four events (Table I): (i) the quasi-molecular ion $[M-H]^-$ progressively lost FH down to the ion $[BP]^- = [M-a-3\times FH]^-$; (ii) during this course, the ion $[M-a]^-$ represented the first ion due to the loss of a side-chain fragment, a, which in turn lost FH down to $[BP]^-$; (iii) the ion of m/z 384 $= [M-h-2\times FH]^- =$

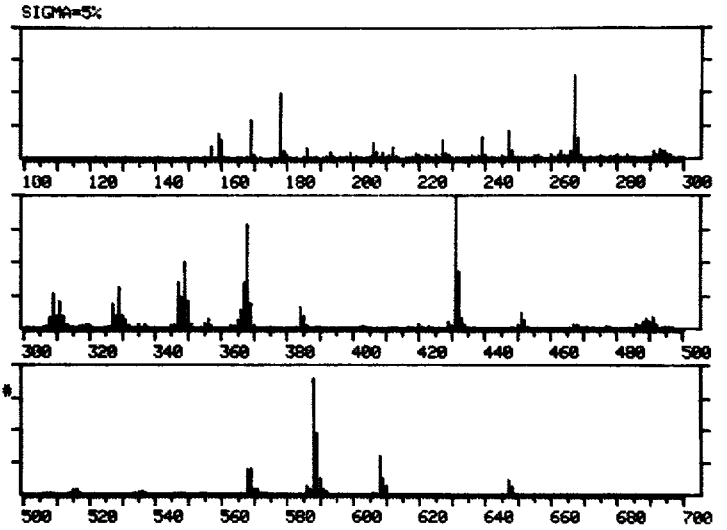

Fig. 4. Ammonia negative ion mass spectrum of the active metabolite **II**-DilBHFB: $[M-H]^- = m/z$ 647.

$[M-224-40]^-$ was the first side-chain fragment common to the three compounds, leading to the ion of m/z 368 $= [M-d]^-$, which in turn was the origin of a series of eleven ions down to the ion of m/z 212 $= [M-d-(a-H)]^-$; and (iv) from the ion of m/z 384 down to the smallest ion of m/z 159 $= [C_4F_7CO-2\times F]^-$, eighteen ions were common to the two drugs, including the ion of m/z 169 $= [C_3F_7]^-$, the only fluorocarbon produced.

Mass fragmentography

Mass fragmentography at the ng, pg and sub-pg levels

The use of an I.S. of the same family as the drug provides two main advantages, first, an identical mechanism of fragmentation into ion families, and second, facilities for establishing the best adjustments of the ionization source and reactant gas. The loss of $3\times FH$ proceeded from either the M^- or $[M+H]^-$ ion, producing either $[M-3\times FH]^- = m/z$ 588 and 574 or $[M+H-3\times FH]^- = m/z$ 589 and 575 from **II**-IBHFB and **III**-IBHFB, respectively. These cleavages were mainly dependent on the ammonia pressure in the ionization source. Owing to the very similar structures of **II** and **III**, the ammonia pressure was easily set in the plateau of the curve which correlates the intensity of ionization to ammonia pressure in the source and where the ionization mechanisms and yields are identical for the compounds. Therefore, one can adjust this pressure in order that the ion $[M-3\times FH]^-$ becomes a base peak for the sake of MF. In addition, in the negative ionization mode the biological matrix elicited less contaminating ions than in the positive ionization mode. Therefore, the double derivatization improves this favourable situation, as the heptafluorobutyryl anhydride reagent allowed many biological components which were only derivatized by *sec*-butanol to be segregated. When comparing the IE, NH_3-CI^+ and NH_3-CI^- modes, the ioniza-

TABLE I

MAIN FRAGMENTS OR ADDUCT IONS PRODUCED BY EI AND POSITIVE AND NEGATIVE MODES OF NH_3-CI FROM THE ISOBUTYL ESTER HEPTAFLUOROBUTYRAMIDE DERIVATIVES OF **II**, THE ACTIVE METABOLITE, AND **III**, THE INTERNAL STANDARD

Electron impact: **II**-(IBHFB)		Positive NH_3-CI: **II**-(IBHFB)		Negative NH_3-CI			
				m/z (RI, %)			
m/z (RI, %)	Origin	*m/z* (RI, %)	Origin	**II**-(IBHFB)	**III**-(IBHFB)	Origin	
648* (1)	M^+	649* (50)	$[M+H]^+$	647* (11)	633* (8)	$[M-H]^-$	
575* (2)	$[M-o]^+$	493* (12)	$[(M+H)^+-(a-H)]^+$	608* (27)	594* (10)	$[M-2\times FH]^-$	
547* (3)	$[M-j]^+$	424* (2)	$[M-h]^+=g^+$	588* (92)	574* (75)	$[M-3\times FH]^-$	
424 (11)	$[M-h]^+$	*387* (21)	$[(M+H)-h-2\times F]^+$	568* (20)	554* (11)	$[M-4\times FH]^-$	
340 (35)	$[M-f-(sb_1-1)]^+$	*370* (6)	$[(M+H)-(d-H)]^+$	491* (8)	477* (8)	$[M-a]^-$	
294 (21)	$[M-f-(j_1+1)]^+$	352 (6)	-	451* (11)	437* (5)	$[M-a-2\times FH]^-$	
281* (54)	$[M-(c-H)]^+$	340* (3)	$[M-f-(j_1-H)]^+$	431*(100)	417*(100)	$[BP]^-=[M-a-3\times FH]^-$	
268 (20)	$[M-d-(j_1-H)]^+$	282* (63)	$[(M+H)-(c-H)]^+$	*384* (17)	*384* (9)	$[M-h-2\times FH]^-$	
252* (5)	$[M-e]^+=f^+$	226* (20)	$[(M+H)-(g-H)]^+$	*368* (80)	*368* (60)	$[M-d]^-=c^-$	
226 (22)	-	224* (38)	$[M-g]^+=f^+$	*349* (52)	*349* (39)	$[M-d-F]^-$	
224*(100)	$[M-g]^+=h^+$	124*(100)	$[BP]^+=[(M+H)-g-j_2]^+$	*347* (36)	347 (23)	$[(M-H)-d-FH]^-$	
168* (30)	$[h-(sb_2-H)]^+$			*329* (27)	329 (23)	$[M-d-FH-F]^-$	
151* (6)	$[h-o_2]^+$			*327* (21)	*327* (12)	$[(M-H)-d-2\times FH]^-$	
124*(100)	$[BP]^+=[h-(j_2-H)]^+$			*311* (28)	*311* (21)	$[M-d-sb_1]^-$	
				309 (26)	*309* (21)	$[M-d-2\times FH-F]^-$	
				293 (5)	*293* (5)	$[M-d-F-(sb_1-H)]^-$	
				291 (4)	*291* (4)	$[M-d-FH-sb_1]^-$	
				267 (62)	*267* (75)	$[M-d-j_1]^-$	
				247 (21)	*247* (30)	$[M-d-j_1-FH]^-$	
				239 (17)	*239* (35)	$[M-f-a]^-$	
				227 (15)	*227* (27)	$[M-d-j_1-2\times FH]^-$	
				212 (6)	*212* (12)	$[M-d-(a-H)]^-$	
				178 (50)	*178* (45)	$[k-F]^-$	
				169 (29)	*169* (17)	$1^-=[C_3F_7]^-$	
				159 (20)	*159* (17)	$[k-2\times F]^-=[C_4F_7O]^-$	

*Corresponding negative ions between **II**-IBHFB and **III**-IBHFB: (647*), homologous perhydroindole ions; (384), identical side-chain ions.

tion currents of the total mass spectrum and of the selected highest mass of **II**-IBHFB were, respectively, IE, $17.1 \cdot 10^6$ and $0.9 \cdot 10^6$; NH_3-CI^+, $4.3 \cdot 10^6$ and $0.24 \cdot 10^6$; and NH_3-CI^-, $37 \cdot 10^6$ and $1.9 \cdot 10^6$, for 60 ng injected (the ionization intensities of **III**-IBHFB being around half of that in the three modes). In the NH_3-CI^- mode the mass spectrometer gain was 10^{-6} instead of 10^{-7} in the other modes. Fig. 5 shows mass fragmentograms of the two plasma-extracted drugs for 1 ng injected and Fig. 6 mass fragmentograms for 20 pg injected, at a gain of 10^{-6}. The upper lanes correspond to the selected ions of **II**-IBHFB, i.e.,

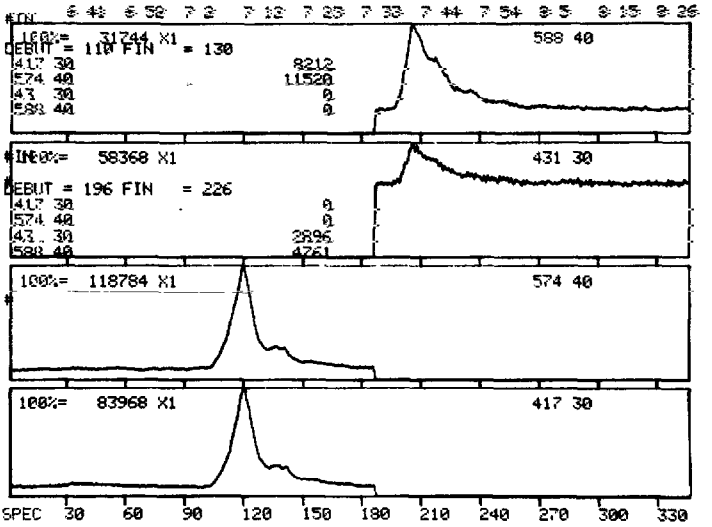

Fig. 5. Mass fragmentogram of **II**-IBHFB and **III**-IBHFB from plasma spiked with 20 pg/ml **II** and 200 pg/ml **III**. NH_3-CI^- at 0.54 Torr of NH_3; source temperature, 150°C.

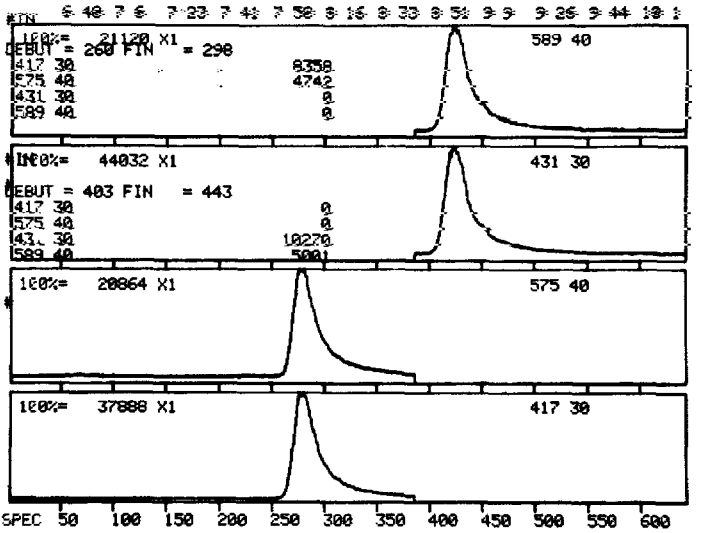

Fig. 6. Mass fragmentogram of **II**-IBHFB and **III**-IBHFB from plasma spiked with 1 ng/ml **II** and 1 ng/ml **III**. Conditions as in Fig. 5.

TABLE II

VALUES OF RESPONSE FACTORS k_i FOR VARIOUS AMOUNTS OF II-IBHFB AND III-IBFHB FOR THE TWO SELECTED IONS OF THE SAME COMPOUND OR THE TWO HOMOLOGOUS IONS BETWEEN EACH COMPOUND

$n = 6$ for each assay.

Amount injected	III-IBHFB 417.30/575.40	II-IBHFB 431.30/589.40	II-IBHFB and III-IBHFB	
			431.30/417.30	589.40/575.40
1 ng	1.789 ± 0.029 (±1.62%)	2.014 ± 0.034 (±1.69%)	1.177 ± 0.077 (±6.54%)	1.047 ± 0.036 (±3.44%)
100 pg	1.723 ± 0.048 (±2.78%)	1.967 ± 0.060 (±3.05%)	1.130 ± 0.050 (±4.42%)	0.992 ± 0.059 (±5.95%)
10 pg	1.751 ± 0.368 (±21.01%)	1.947 ± 0.218 (±11.20%)	1.075 ± 0.141 (±13.11%)	0.951 ± 0.101 (±10.62%)

589.40 = $[(M+H)-3\times FH]^-$ and 431.30 = $[BP]^+ = [M-a-3\times FH]^-$. The detection limit was 600 fg injected with a signal-to-noise ratio of 3 for the ions of m/z 575.40 and 417.30 of **III**-IBHFB and 589.40 of **II**-IBHFB.

Mass fragmentography performance

Response factors, k_i, were calculated from the peak areas of the selected ions. Calibration graphs were established with increasing amounts of **II** versus a constant amount of **III** (see Method of plasma assay). The constancy of k_i, which depends on the stability of the mass spectrometer and the ammonia pressure in the source, was regularly checked. Table II shows the k_i values for 1 ng, 100 pg and 10 pg injected. MF assays under the described conditions were excellent for 1 ng and 100 pg injected, as shown by the coefficients of variation (C.V.): from 1.62 to 6.54% for 1 ng and from 2.78 to 5.95% for 100 pg. The dispersion was still acceptable for 10 pg (from 10.62 to 21.01%). It must be pointed out that the use of **III** as the I.S. reduced the variations among the three samples, as shown by the last two columns in Table II: from 6.54 to 13.11% for the three ratios of the ions of m/z 431.30 and 417.30 and from 3.44 to 10.62% for those of the ions of m/z 589.40 and 575.40. However, it was observed that when assaying together **II**-IBHFB, the active metabolite and **I**-IBHFB, the parent drug, the ethyl ester of the parent drug (Fig. 1A) was partially transesterified into the isobutyl ester. The formation of isobutyl ester derivatives being dependent on the concentration of hydrochloric acid in isobutanol, attempts were made to decrease it. However, kinetic studies did not permit a lower concentration of hydrochloric acid to be found which could achieve complete esterification of the free carboxylic groups without any transesterification. Therefore, to overcome this situation, other types of derivatization were tried, and trimethylsilyl derivatization of the free carboxylic group(s) alone was selected.

Trimethylsilyl derivatives

Gas chromatography

The kinetics of derivatization with BSA, which was found to be the most suitable silylating reagent, showed complete esterification of the unique carboxylic group of **I** and the two of **II** and **III** using BSA–pyridine (50:50, v/v) at 60°C for 2 h, without any effect on the amino group, which remained free. The derivatization kinetics as a function of heating duration were followed by calculating k_i from peak-area ratios for each drug versus a constant amount of *n*-triacontane, which is not derivatized. Fig. 7 shows a typical gas chromatogram and the order of elution of **III**-diTMS (I), **I**-monoTMS (II), **II**-diTMS (III) and *n*-triacontane (IV).

Gas chromatography–mass spectrometry

In the EI mode the three compounds were highly fragmented and the mass spectra were very poor, showing only the base peak arising from the side-chain cleavage (Fig. 8) into ions of m/z 172 for **I**-monoTMS (Fig. 8A) and 216 for **II**-diTMS (Fig. 8B) and **III**-diTMS (Fig. 8C). The $[M-15]^+$ ions of the three

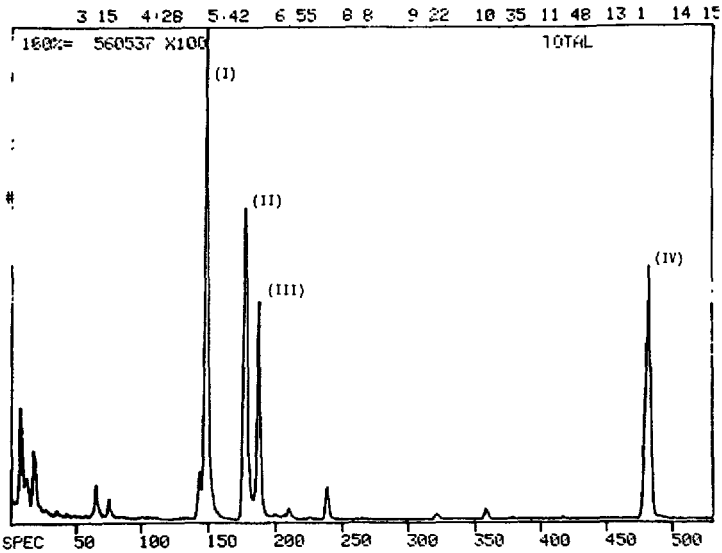

Fig. 7. Gas chromatography of a mixture of (I) **III**-diTMS (I.S.), (II) **I**-monoTMS, (III) **II**-diTMS and (IV) *n*-triacontane. Conditions as in Fig. 2.

compounds had RI below 1%. A third type of cleavage gave on the one hand $[M-117]^+ = [M-OCOSi(CH_3)_3]^+ = m/z$ 353 (RI=15%) for **III**-diTMS and 367 (RI=7%) from **II**-diTMS and on the other hand $[M-73]^+ = m/z$ 367 (RI=8%) for **I**-monoTMS (Table III). These ions may arise from the cleavage of the bond between the carbethoxy and butylamino moieties, as **I**-monoTMS did not release any ion of m/z 117 from the ring TMS ester and the diTMS esters of the two other drugs diTMS not give any ion of m/z 73, i.e. $[Si(CH_3)_3]^+$ (see Table III and Fig. 8). In the NH_3-CI^+ mode the mass spectra showed mainly a base peak of the adduct ion $[M+H]^+$ of m/z=471 for **III**-diTMS, 441 for **I**-monoTMS and 485 for **II**-diTMS. However, no other important ions were found except the side-chain ions of m/z 216 and 172, respectively (RI≈18%). In the CH_4-CI^+ mode the mass spectra of the three compounds displayed at least six ions, $[M+H]^+$, $[M-15]^+$, $[M-117]^+$ or $[M-73]^+$, $[BP]^+$ and the characteristic adduct ion $[M+29]^+$. Table III lists these fragmentations and relative intensities. It shows that selected ions for performing MF can be $[M+H]^+$ and $[BP]^+ = [\text{side-chain}]^+$ for each compound, i.e., ions of m/z 471 and 216 for **III**-diTMS, 441 and 172 for **I**-monoTMS and 485 and 216 for **II**-diTMS. Following the injection of 10 ng of **III**-diTMS, **I**-monoTMS and **II**-diTMS, the total ionization current was proportional and averaged, respectively, (i) $4.9 \cdot 10^5$, $4.3 \cdot 10^5$ and $1.9 \cdot 10^5$ in the EI mode and (ii) $0.72 \cdot 10^5$, $0.68 \cdot 10^5$ and $0.30 \cdot 10^5$ and $0.30 \cdot 10^5$ in the CH_4-CI mode. The values for the CH_4-CI mode were 2.0, 1.6 and 1.7 times higher than in the NH_3-CI mode, respectively. The total ionization yields in the CH_4-CI mode versus IE were 14.6%, 15.8% and 15.7% for **III**-diTMS, **I**-monoTMS and **II**-diTMS, respectively.

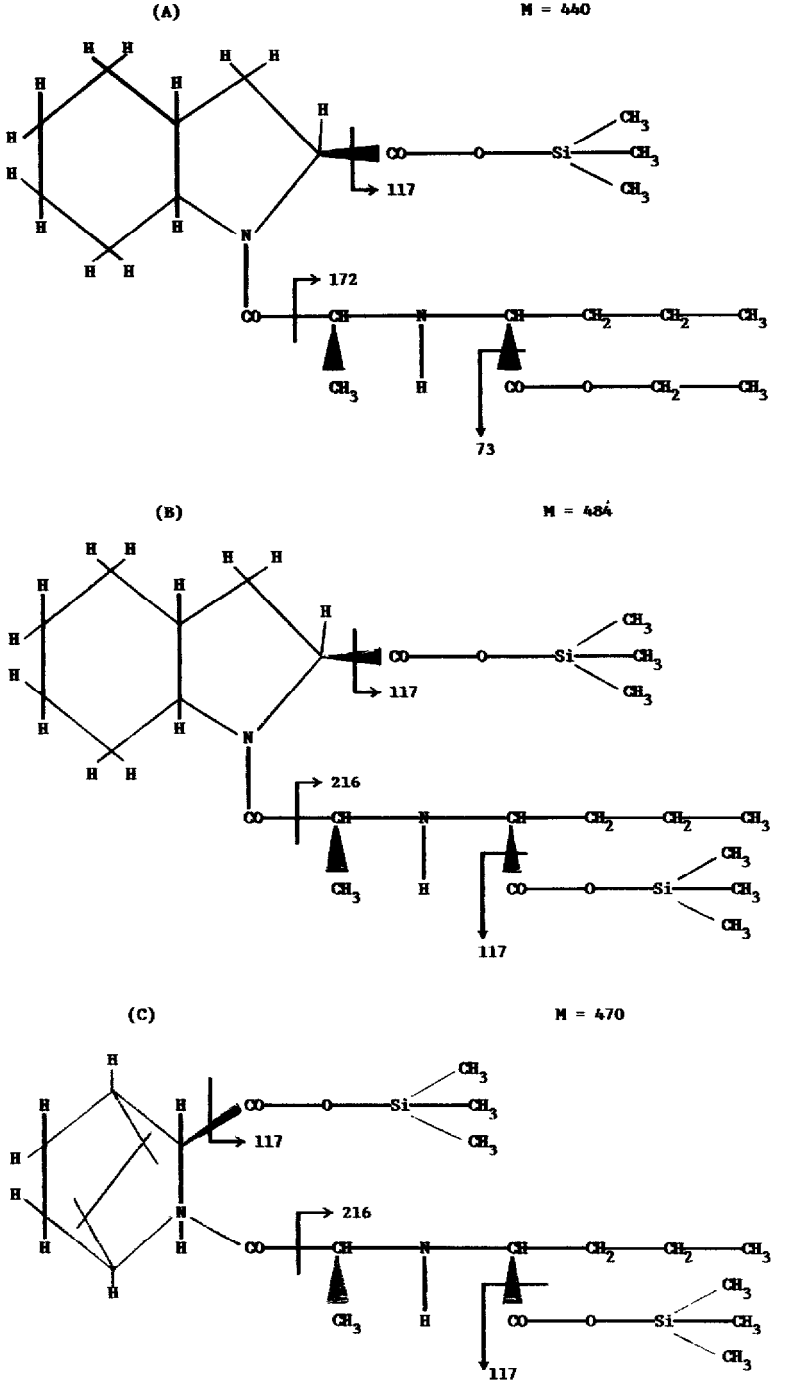

Fig. 8. Structure and fragmentation of Perindopril (A), the active metabolite (B) and the I.S. (C) as TMS derivatives.

TABLE III

MAIN FRAGMENTS AND ADDUCT IONS PRODUCED BY CH_4-CI FROM THE TMS ESTERS OF III, I AND II

Origin	*m/z* (RI, %)		
	III-diTMS	I-monoTMS	II-diTMS
$[M+29]^+$	499 (2)	469 (2)	513 (1)
$[M+H]^+$	471 (100)	441 (100)	485 (95)
$[M-15]^+$	455 (31)	425 (17)	469 (33)
$[M-OCOTMS]^+$	353 (25) = $[M-117]^+$	-	367 (15) = $[M-117]^+$
[M−73]	-	367 (8)	-
[Side-chain]$^{+a}$	216 (100)	172 (92)	216 (100)

[a]Side-chain is $-CH(CH_3)NHCH(C_3H_7)COOR$, where R is $-Si(CH_3)_3$ for III-diTMS and II-diTMS and by $-CH_2CH_3$ for I-monoTMS.

Mass fragmentography

Chemical ionization parameters

Because the total ionization current of the TMS derivatives were much lower in the CH_4-CI^+ mode than those of IBHFB derivatives in the NH_3-CI^- mode, careful setting and control of the ionization source were essential. The electron energy of the filament was set between 60 and 70 eV, for which the selected ion ratios, $[M+H]^+/[\text{side-chain}]^+$, were 0.50 to 0.85 without loss of sensitivity. The source temperature was set at 140°C to prevent heavy pollution and frequent cleanings. Ionization ratios, $[M+H]^+/[\text{side-chain}]^+$, were plotted against methane pressure in the source. The ratios were close to 1 at $7 \cdot 10^{-2}$ Torr, without much variation between $9 \cdot 10^{-2}$ and $5 \cdot 10^{-2}$ Torr.

Extraction yields and reproducibility

Extraction yields were calculated from five assays on each drug, considering one drug as an external standard. Plasma samples were spiked with two drugs at two equal concentrations (10 or 500 ng/ml) and then extracted. The third drug was added at the same concentration before carrying out MF assays. The coefficients of variation ($n=3$ or 4), were between 10 and 25% for the low concentration (10 ng/ml) and between 5 and 10% for the high concentration (500 ng/ml). The reproducubility was established in the same way on three aliquots of two plasmas samples containing 10 or 500 ng/ml of I and II using III as the external standard. The extraction yields were between and 15% for 500 ng/ml and 8–12% for 10 ng/ml.

Precision of mass fragmentography assays

Intra-day and inter-day reproducibility of k_i. Comparisons were carried out by MF on plasma samples spiked with 10 ng/ml of I and II. These plasma samples were divided into three aliquot fractions, each being assessed four times a day during four days. The intra-day reproducibility was between 5.6 and 8.6% for I

(6.8±0.7%) and between 2.9 and 9.9% for **II** (5.8±1.5%). The inter-day reproducibility was between 2.3 and 5.7% for **I** (4.4±1.1%) and between 3.7 and 11.6% for **II** (6.6±2.5%).

Intra-assay and inter-assay reproducibility. Three batches of plasma were spiked with three different concentrations (5, 50 or 500 ng/ml) of **I** and **II** and were divided into five aliquot fractions, which were assessed by MF using **III** as I.S. The intra-assay reproducibility was between 3.3 and 6.7% for **I** and between 3.7 and 13.8% for **II**. The inter-assay reproducibility was between 11 and 12% for **I** (11.6±5.2%), whatever the drug concentrations, and 8, 13 and 22% for **II** at concentrations of 500, 100 and 10 ng/ml, respectively.

Accuracy of mass fragmentography assays

Calibration graph linearity. The four calibration graphs, CG-1 to CG-4, were established by MF according to the above procedure using the selected ions $[M+H]^+$ of **I** (m/z 441) and **II** (m/z 485) versus **III** (m/z 471). Table IV shows the regression equations, where x is the amount of **I** or **II** in ng/ml and y represents peak-area ratios of the $[M+H]^+$ ions of **I**-monoTMS and **II**-diTMS to the $[M+H]^+$ ion of **III**-diTMS. There is excellent linearity of the eight regression curves of the four calibration graphs, the correlation coefficient, r, in most instances being better than 0.9990 and at a high level of confidence, $p<0.001$, in each instance.

Assays of known spiked plasma samples. Plasma samples spiked off with 10 ng/ml of **III** and increasing amounts of **I** and **II** (0.100, 1, 10, 30, 100, 250 and 500 ng/ml) were submitted to MF assessment. All mass fragmentograms demonstrated the excellent separativity and sensitivity of the method, as demonstrated by Fig. 9, which shows a mass fragmentogram of the lowest concentration in CG-1: 100 pg/ml of **I** and **II** and 1 ng/ml of **III** for 1 μl injected. The arrows on the upper three traces indicate from bottom to top, the ions monitored, $[M+H]^+$ m/z=471.40, 441.40 and 485.40, and $[BP]^+$ m/z=216.30, 172.20 and 216.30, for

TABLE IV

REGRESSION EQUATIONS OF THE FOUR CALIBRATION GRAPHS FOR THE TMS ESTERS OF I AND II

Calibration graph	Compound	Selected ions[a]	Ion area ratio (y)[b]	Correlation coefficient (r)	p
CG-1	**I**	441/471	$y=0.042x+0.015$	0.9999	<0.001
	II	485/471	$y=0.021x+0.024$	0.9995	<0.001
CG-2	**I**	441/471	$y=0.054x+0.121$	0.9999	<0.001
	II	485/471	$y=0.044x+0.033$	1.0000	<0.001
CG-3	**I**	441/471	$y=0.057x+0.260$	0.9973	<0.001
	II	485/471	$y=0.055x+0.580$	0.9980	<0.001
CG-4	**I**	441/471	$y=0.042x+0.092$	0.9991	<0.001
	II	485/471	$y=0.039x+0.400$	0.9962	<0.001

[a]Selected ions: $[M+H]^+$, m/z=441 of **I**-monoTMS, 475 of **II**-diTMS and 471 of **III**-diTMS.
[b]x=concentration of **I** or **II**.

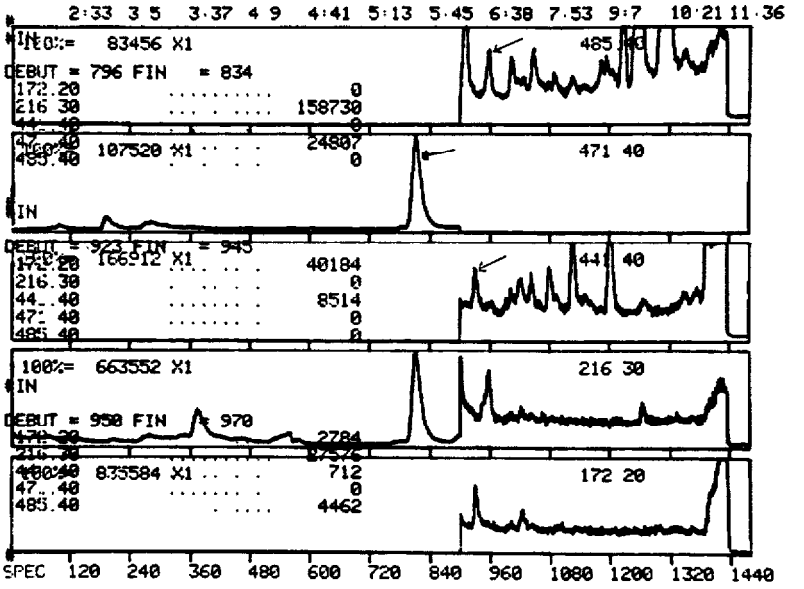

Fig. 9. Mass frgmentogram of I-monoTMS and II-diTMS from plasma spiked with 100 pg/ml each and 1 ng/ml of III-diTMS (I.S.).

III-diTMS, I-monoTMS and II-diTMS, respectively. From these data it can be concluded that on routine daily and day-to-day schedules the limit of detection of I and II is 100 pg/ml, i.e., 1–2 pg injected, and that the limit of sensitivity is ca. 1–2 ng/ml, taking into account the inherent amplification of variations of the biological matrix when several hundred assays have to be completed to establish plasma elimination curves. Therefore, the accuracy and precision can be improved for a limited number of assays using a well conditioned column and a clean mass spectrometer.

Assays of unknown spiked plasma samples. Samples with different plasma concentrations from the calibration graph CC-3 were treated as unknown samples using mean k_i values from three reference plasma samples. Assays were carried out for I and II on $[M+H]^+$ ions for six concentrations (2.5, 10, 30, 50, 250 and 500 ng/ml). The mean accuracy was $12 \pm 2\%$ ($n=12$) for I-monoTMS and $15 \pm 3\%$ ($n=12$) for II-diTMS.

CONCLUSION

Perindopril is an example of a parent drug that releases a metabolite acting at low levels. The first MF method, despite showing good separations and sensitivity owing to complete derivatization of the amino group into the heptafluorobutyramide and of carboxylic groups into the isobutyl ester, could not be applied to the assessment of plasma spiked with I and II together. However, the optimization of a less efficient method in terms of sensitivity, precision and accuracy when using the TMS derivative of carboxylic groups only, allowed the analytical requirements for biological samples to be met, viz., a sensitivity of 1–2 ng/ml of

plasma, a precision showing reproducibilities of 2.9–9.9% intra-day, 2.3–11.6% inter-day, 3.3–13.8% intra-assay and 8–22% inter-assay, and an accuracy of 12–15%. New pharmaceutical xenobiotic drugs are designed to act as effectors at defined sites of metabolic pathways. More specifically, they are administered in low doses. Pharmacokinetics depend on assays of parent drugs, metabolites and conjugates at very low levels (ng/ml or less) in plasma. Metabolic transformations are at the origin of chemical and biological interferences during the analytical process, such as chemical transformations and immunological cross-reactions. Immunopharmacology is a developing field; immunoassays are becoming increasingly sensitive and compete efficiently with physico-chemical separation methods and the immunoreactions and immunotoxicity of drugs are beginning to be understood. They are suspected of arising from drug-directed antibodies where the antigen resulted from an irreversible exchange of the drug from its glucuronide to a free amino group of a plasma protein which become immunogenic [8]. The evolution of analytical pharmacology will take advantage of the development of combined physico-chemical and immunological methods.

REFERENCES

1 M. Vincent, G. Rémond, B. Portevin, B. Serkiz and M. Laubie, Tetrahedron Lett., 23 (1982) 1677.
2 M. Laubie, P. Schiavi, M. Vincent and H. Schmitt, J. Cardiovasc. Pharmacol., 6 (1984) 1076.
3 S. Fournel-Gigleux, J. Magdalou, C. Lafaurie, G. Siest, L. Grislain, M.H. Garnier, J.F. Dabe, W. Luijten, N. Bromet and M. Devissaguet, in G. Siest, J. Magdalou and B. Burchell (Editors), Cellular and Molecular Aspects of Glucuronidation, Colloque INSERM/John Libbey Eurotext, London, 1988, p. 79.
4 O.H. Drummer, K. Rowley, H. Johnson, P. Worland, B. Workman, G.L.G. Harris, E.L. Conway and W.L. Louis, Excerpta Med., 750 (1987) 545.
5 J. Desgrès, D. Boisson and P. Padieu, J. Chromatogr., 162 (1979) 133.
6 A. Ros, J. Gas Chromatogr., 3 (1965) 252.
7 C. Tsaconas, P. Padieu, G. Maume, M. Chessebeuf, N. Hussein and N. Pitoizet, Anal. Biochem., 157 (1986) 300.
8 L.Z. Benet and H. Spahn, in G. Siest, J. Magdalou and B. Burchell (Editors), Cellular and Molecular Aspects of Glucuronidation, Colloque INSERM/John Libbey Eurotext, London, 1988, p. 261.